Enzymatic Degradation Processes of Poly[(*R*)-3-hydroxybutyric acid] and Poly[(*R*)-3-hydroxybutyric acid-*co*-(*R*)-3-hydroxyvaleric acid] Single Crystals Revealed by Atomic Force Microscopy: Effects of Molecular Weight and Second-Monomer Composition on Erosion Rates

Keiji Numata,[†] Yoshihiro Kikkawa,[‡,§] Takeharu Tsuge,[†] Tadahisa Iwata,[‡] Yoshiharu Doi,[†,‡] and Hideki Abe*[,†,‡]

Department of Innovative and Engineered Materials, Tokyo Institute of Technology, 4259 Nagatsuta, Midori-ku, Yokohama 226-8502, Japan, Polymer Chemistry Laboratory, RIKEN Institute, 2-1 Hirosawa, Wako-shi, Saitama 351-0198, Japan, and Nanoarchitectonics Research Center, National Institute of Advanced Industrial Science and Technology (AIST), Tsukuba Central 4, 1-1-1 Higashi, Tsukuba, Ibaraki 305-8566, Japan

Received February 14, 2005; Revised Manuscript Received April 15, 2005

Enzymatic degradation processes of poly[(*R*)-3-hydroxybutyric acid] (P(3HB)) and poly[(*R*)-3-hydroxybutyric acid-*co*-(*R*)-3-hydroxyvaleric acid] (P(3HB-*co*-3HV)) single crystals in the presence of PHB depolymerase from *Ralstonia pickettii* T1 were studied by real-time and static atomic force microscopy (AFM) observations. Fibril-like crystals were generated along the long axis of single crystals during the enzymatic degradation, and then the dimensions of fibril-like crystals were analyzed quantitatively. The morphologies and sizes of fibril-like crystals were dependent on the molecular weight and copolymer composition of polymers. For all samples, the crystalline thickness gradually decreased toward a tip from the root of a fibril-like crystal after enzymatic degradation for 1 h. The thinning of fibril-like crystals may be attributed to the destruction of chain-packing structure toward crystallographic *c* axis by the adsorption of enzyme. From the real-time AFM images, it was found that at the initial stage of degradation the enzymatic erosion started from the disordered chain-packing region in single crystals to form the grooves along the *a* axis. The generated fibril-like crystals deformed at a constant rate along the *a* axis with a constant rate after the induction time. The erosion rate at the grooves along the *a* axis increased with a decrease of molecular weight and with an increase of copolymer composition. On the other hand, the erosion rate along the *a* axis, at the tip of the fibril-like crystal, was dependent on only the copolymer composition, and the value increased with an increase in the copolymer composition. The morphologies and sizes of fibril-like crystals were governed by both the erosion rates along the *a* axis at the grooves and tip of fibril-like crystals. In addition, we were able to estimated the overall enzymatic erosion rate of single crystals by PHB depolymerase from the volumetric analysis.

Introduction

Poly(hydroxyalkanoic acids) (PHA) are partially crystallized thermoplastic produced from renewable carbon resources and are biodegradable in the natural environments.[1−3] The crystal structure of poly[(*R*)-3-hydroxybutyric acid] (P(3HB)) is orthorhombic form with unit cell parameters: $a = 0.576$ nm, $b = 1.320$ nm, and c (fiber axis) $= 0.596$ nm and space group of $P2_12_12_1$.[4,5] The conformational analysis by intermolecular energy calculation has indicated that the P(3HB) molecule has a left-handed 2_1 helix conformation.[5−8]

The biodegradability of PHA has been reported in a number of papers.[9−13] PHA is hydrolyzed by poly(hydroxybutyric acid) (PHB) depolymerases secreted from microorganisms.[9−12] The PHB depolymerase from *Ralstonia pickettii* T1 (formally *Alcaligenes faecalis* T1) used in this study has three characteristic domains, e.g., catalytic, binding, and linker domains, and the molecular weight is 47 000.[9,12] PHB depolymerase from *R. pickettii* T1 was observed directly by atomic force microscopy (AFM), and the average dimensions were 4.4 nm in height and 19 nm in width on poly(l-lactide) thin film.[13] PHB depolymerase was shown to adhere on P(3HB) crystalline regions and preferentially degraded the polymer chain in amorphous regions.[14]

To elucidate the mechanism of enzymatic hydrolysis of PHA materials with PHB depolymerases, the enzymatic reaction has been actively investigated using films and single crystals of PHA. It has been demonstrated that the rate of biodegradation for PHA materials is strongly dependent both on the chemical structure of monomeric units and on the solid-state structure of samples.[14] In the aspect of the solid-

* To whom correspondence should be addressed. Phone: +81-48-467-9404. Fax: +81-48-462-4667. E-mail: habe@riken.jp.
[†] Tokyo Institute of Technology.
[‡] RIKEN Institute.
[§] National Institute of Advanced Industrial Science and Technology (AIST).

10.1021/bm0501151 CCC: $30.25
Published on Web 05/12/2005

Table 1. Molecular Weights and Optimal Crystallization Conditions of PHA Samples Used in This Study

	molecular weights[b]		crystallization conditions		
sample[a]	number-average molecular weight $M_n \times 10^{-3}$ g/mol	polydispersity M_w/M_n	concentration (w/v) %	$CHCl_3/CH_3OH$ (v/v)	crystallization temperature (°C)
H−P(3HB)	240	2.2	0.025	1/7	77
M−P(3HB)	55	1.7	0.025	1/7	76
L−P(3HB)	8.5	1.4	0.025	1/7	60
P(3HB-*co*-6 mol % 3HV)	51	1.6	0.029	1/13	65
P(3HB-*co*-14 mol % 3HV)	33	1.5	0.029	1/13	60

[a] H-, high molecular weight; M-, medium molecular weight; L-, low molecular weight. [b] Molecular weights were determined by GPC.

state structure of PHA materials, the crystallinity and lamellar crystal sizes play a decisive role in the degradation process.

PHA single crystals have been used to elucidate the enzymatic degradation behavior of the crystalline phase in lamellar crystals.[15−23] Hocking et al. carried out enzymatic degradation of P(3HB) single crystal by PHB depolymerase and reported preferential degradation from the crystal edges.[15] Nobes et al., using transmission electron microscopy (TEM), found conversion of PHA single crystals into a needlelike morphology after enzymatic degradation, and suggested an "edge attack" mechanism.[16,17] Iwata et al. also used TEM to along with an immuno-gold labeling technique to investigate the enzymatic degradation of PHA single crystals and the adsorption of PHB depolymerase and found that PHB depolymerase adsorbed on the crystalline surface unselectively and degraded lamellar crystal along the crystallographic *a* axis from the crystal edges and ends.[18−20] Recently, on the basis of AFM observations, Murase et al. have proposed that straight degradation pathways exist in P(3HB) single crystals along the *a* and *b* axes, resulting in the formation of slits and crevices during enzymatic degradation.[21,22] Moreover, using a mutant enzyme disrupted in its hydrolytic activity, they demonstrated that the adsorption of PHB depolymerase onto the crystalline surface disturbed the molecular packing of P(3HB) single crystals.[23]

In our previous report,[24] the enzymatic degradation processes of flat-on lamellar crystals in melt-crystallized thin films of PHA were characterized by real-time AFM in a phosphate buffer solution of PHB depolymerase from *R. pickettii* T1. Fibril-like crystals with regular intervals were generated along the *a* axis at the end of lamellar crystals during enzymatic degradation, and the sizes of fibril-like crystals were analyzed quantitatively. The lamellar morphologies of fibril-like crystals depended on the copolymer composition of PHA samples. The width and thickness decreased at the tip of fibril-like crystals, indicating that the enzymatic degradation takes place not only along the *a* axis but also along the *b* and *c* axes. In addition, the erosion rates along the *a* axis of flat-on lamellar crystals were determined from real-time AFM observations. On the basis of the AFM observations, a glacial destruction model for the enzymatic degradation of lamellar crystals of P(3HB) by PHB depolymerase was proposed.

In this study, we prepared five samples of PHA single crystals from both P(3HB) with different molecular weights and poly[(*R*)-3-hydroxybutyric acid-*co*- (*R*)-3-hydroxyvaleric acid] (P(3HB-*co*-3HV)) (3HV = 6 and 14 mol %) with different compositions, and the enzymatic degradation processes of PHA single crystals were carried out in the presence of PHB depolymerase from *R. pickettii* T1. The morphology of fibril-like crystal formed during enzymatic degradation was characterized by static AFM, and the dimensions of fibril-like crystals were analyzed quantitatively. In addition, we performed real-time AFM during enzymatic degradation of single crystals, and the enzymatic erosion rates of PHA single crystals were evaluated.

Materials and Methods

Preparation of PHA Single Crystals. Poly[(*R*)-3-hydroxybutyric acid] (P(3HB)), poly[(*R*)-3-hydroxybutyric acid-*co*-6 mol % (*R*)-3-hydroxyvaleric acid] (P(3HB-*co*-6mol % 3HV)), and poly[(*R*)-3-hydroxybutyric acid-*co*-14 mol % (*R*)-3-hydroxyvaleric acid] (P(3HB-*co*-14mol % 3HV)) were prepared by microbial synthetic methods.[1,2] Alkali hydrolysis of P(3HB) ($M_n = 240 \times 10^3$), P(3HB-*co*-6mol % 3HV) ($M_n = 120 \times 10^3$), and P(3HB-*co*-14mol % 3HV) ($M_n = 130 \times 10^3$) were performed to obtain the single crystals with good folding regularity according to the method reported previously.[17] Three P(3HB) samples with different molecular weights were prepared as H−P(3HB) ($M_n = 240 \times 10^3$), M−P(3HB) ($M_n = 55 \times 10^3$), and L−P(3HB) ($M_n = 8.5 \times 10^3$). Two copolymer samples with 6 mol % 3HV and 14 mol % 3HV ($M_n = 51 \times 10^3$ and 33×10^3, respectively) were adopted to prepare single crystals. Single crystals of all PHA samples were grown from dilute solution of a mixture of chloroform and methanol under isothermal crystallization for 12 h. PHA single crystals were collected by decantation and washed with methanol at 25 °C. These PHA single crystals were observed with JEM-2000FXII electron microscope operated at the acceleration voltage of 120 kV for electron diffraction to ensure the crystal structure of PHA single crystals.[17] Table 1 shows molecular weights and crystallization conditions of five PHA samples used in this study. Molecular weights and polydispersities were measured by gel permeation chromatography system (GPC) with polystyrene standards to make the calibration curve.[10]

Enzymatic Degradation Experiment. Extracellar PHB depolymerase from *Ralstonia pickettii* T1 was purified to electrophoretic homogeneity according to the method reported by Shirakura et al.[25] PHA single crystals were deposited on a silicon wafer (10×10 mm^2) and were dried in air. Subsequently, PHA single crystals on the silicon substrate were immersed in 0.1 M potassium phosphate

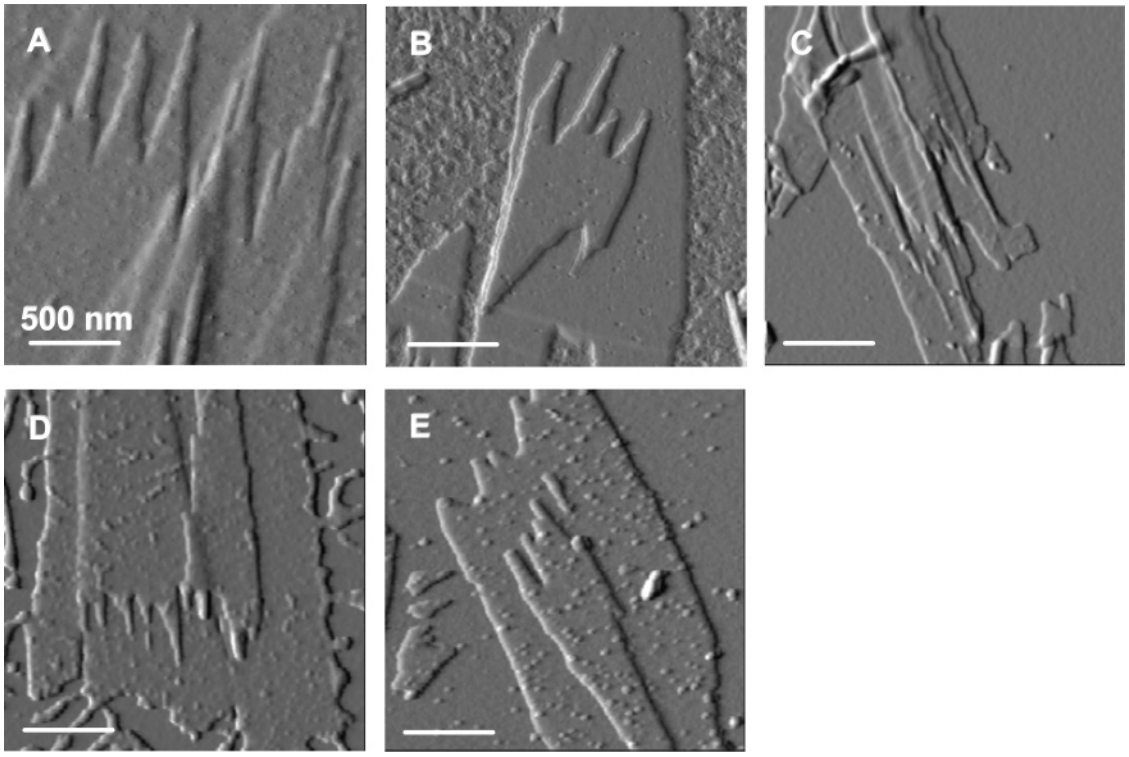

Figure 1. AFM amplitude images of single crystals for H−P(3HB) (A), M−P(3HB) (B), L−P(3HB) (C), P(3HB-*co*-6mol % 3HV) (D), and P(3HB-*co*-14mol % 3HV) (E) after enzymatic degradation by PHB depolymerase for 1 h at 37 °C, respectively. These images were obtained at 25 °C in air. Each scale bar is 500 nm.

buffer (pH 7.4) containing PHB depolymerase and degraded enzymatically at 37 °C for 1 h. The concentration of the enzyme solution was 1.0 μg/mL. After the enzymatic degradation, samples were washed a few times with Milli-Q water and methanol, and were dried at 25 °C for 1 day.

AFM Observation. Enzymatic degradation processes of PHA single crystals were observed by real-time AFM (Seiko Instruments Inc. SPI3800/SPA 300HV) in a phosphate buffer solution containing PHB depolymerase. A 10 × 10 mm splitting of PHA single crystals on the silicon substrate was fixed to the bottom of a reaction vessel (diameter: 25 mm, height: 5 mm). The sample in the vessel was set on the AFM scanner, and 1.5 mL of the phosphate buffer solution was poured into the vessel. Crystalline morphologies before the enzymatic degradations were observed in the phosphate buffer solution at 37 °C. Then, the enzymatic degradation was initiated by addition of concentrated enzyme solution (200 μg/mL) into the phosphate buffer solution in the vessel, resulting in a final concentration of enzyme solution with ca. 1.0 μg/mL. A 400 μm long silicon cantilever with spring constants of 1.5 N/m was adopted in the real-time dynamic force mode (tapping mode) AFM in the phosphate buffer solution at 37 °C. A light tapping force (set-points value = 0.8−0.9) was applied for the AFM observation in the enzyme solution in order to avoid damage on the crystalline surface by the cantilever tip. Height and amplitude images were simultaneously obtained. The calibration of cantilever tip-convolution effect was carried out to obtain the true dimensions of objects by the method described previously.[24]

Results

Quantitative Analysis of PHA Single Crystals during Enzymatic Degradation Measured by Static AFM Observations. Five samples of PHA single crystals were prepared from dilute solutions of chloroform and methanol. The lamellar single crystals were deposited on silicon substrates, and the crystalline morphology was characterized by using AFM. Lath-shaped crystals with dimensions of approximately 1.5 and 10.0 μm along the short and long axes, respectively, were observed for each sample, and the thickness of an individual single-crystal ranged from 5 to 7.0 nm.

By using PHA single crystals mounted on a silicon substrates, the enzymatic degradation was carried out in the presence of PHB depolymerase from *R. pickettii* at 37 °C for 1 h. After enzymatic degradation for 1 h, PHA single crystals were observed by static AFM. Figure 1 shows AFM amplitude images of PHA single crystals after degradation. As shown in each image of Figure 1, fibril-like crystals were formed along the long axis of all single crystals after enzymatic degradation. It seems that both the molecular weight and the monomer secondary composition affect the morphology of fibril-like crystals. The dimensions of fibril-like crystals were analyzed quantitatively from the AFM images. Figure 2 represents the definitions of the appointed dimensions in fibril-like crystals formed after enzymatic degradation.

Table 2 lists the average values of the dimensions of fibril-like crystals defined as Figure 2. For H−P(3HB) single crystals, the average values of the length and interval of fibril-like crystal were 326 ± 230 and 124 ± 66 nm, respectively. The width at the tip of fibril-like crystals for the H−P(3HB) sample was 43 ± 14 nm. The thickness at the root of fibril-like crystals was 6.3 ± 0.7 nm, and the value was almost identical with the thickness of single crystals before degradation. The thickness of the intermediate region of fibril-like

Table 2. AFM Measurements on the Dimensions of P(3HB) Fibril-Like Crystals Generated from Single Crystals after a 1 h Enzymatic Degradation at 37 °C

			width,[a] nm	thickness,[a] nm		
sample	length,[a] nm	interval,[a] nm	tip	root	middle	tip
H−P(3HB)	326 ± 230	124 ± 66	55 ± 15	6.3 ± 0.7	5.3 ± 0.8	3.5 ± 0.9
M−P(3HB)	373 ± 166	125 ± 55	51 ± 18	5.8 ± 0.5	4.9 ± 0.6	2.9 ± 1.0
L−P(3HB)	572 ± 340	130 ± 67	64 ± 17	5.4 ± 0.5	4.5 ± 0.6	2.7 ± 0.8
P(3HB-*co*-6 mol % 3HV)	212 ± 63	88 ± 20	39 ± 11	5.8 ± 0.5	4.9 ± 0.7	2.8 ± 0.8
P(3HB-*co*-14 mol % 3HV)	193 ± 72	85 ± 23	39 ± 11	5.7 ± 0.4	5.2 ± 0.5	2.7 ± 0.7

[a] Each dimension of fibril-like crystal is defined as Figure 2, parts A and B.

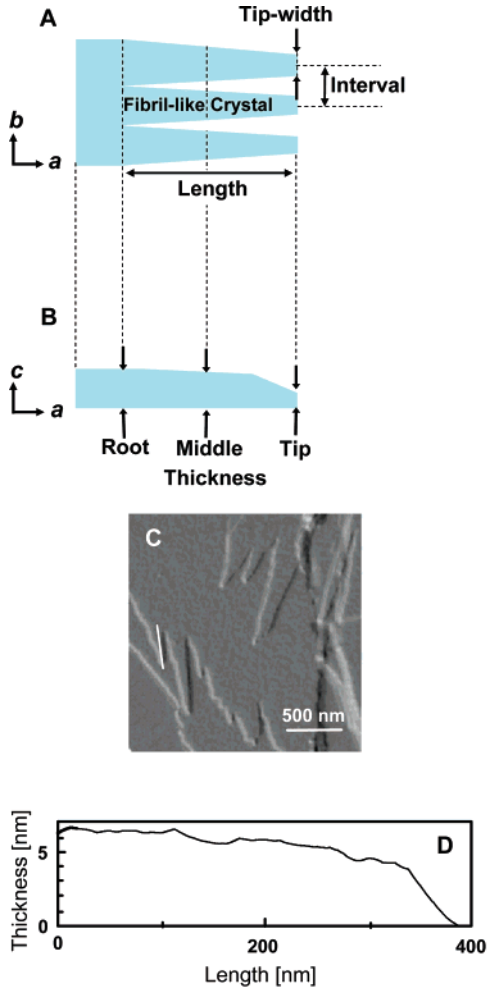

Figure 2. Schematic representations (A and B), AFM amplitude images (C), and cross-section (D) of fibril-like crystals generated from PHA single crystals during enzymatic degradation by PHB depolymerase from *R. pickettii* T1 at 37 °C. Each dimension of the fibril-like crystal is defined as Figure 2A,B. A white line in Figure 2C is the distance of the cross-section shown in Figure 2D.

crystals was slightly decreased compared with the thickness of original single crystals. At the tip of the fibril-like crystals, the crystals apparently became thin, and the average thickness value was 3.5 ± 0.9 nm.

The length of fibril-like crystals were dependent on the molecular weight of P(3HB) samples, and the values became smaller in the following order: L−P(3HB) > M−P(3HB) > H−P(3HB). On the other hand, both the interval and tip-width had relatively similar values, independent of the molecular weight, for all P(3HB) samples. For all P(3HB) samples, the thickness at the root of fibril-like crystals was almost identical with the thickness of single crystals before degradation, and the thickness of fibril-like crystals was gradually thinned toward the tip of the crystal.

Also, for P(3HB-*co*-3HV) samples, the thickness of fibril-like crystals was gradually thinned from the root to the tip of crystal. The thickness at the tip ranged from 2.7 ± 0.7 to 2.8 ± 0.8 nm, and the values were almost the same with those of the P(3HB) samples. The lengths and intervals of the fibril-like crystals for P(3HB-*co*-3HV) samples had relatively similar values, independent of the 3HV composition. The width at the tip of fibril-like crystals for both P(3HB-*co*-6mol % 3HV) and P(3HB-*co*-14mol % 3HV) samples revealed the same value of 39 ± 11 nm. However, all of these values were apparently smaller than those of P(3HB) samples.

It is of interest to note that the fibril-like crystals did not taper completely, and that the crystals with dimensions either of less than 1.9 nm thickness or of less than 28 nm width were not observed for all PHA samples after degradation at 37 °C for 1 h. These minimum values of thickness and width of fibril-like crystals may mean the critical dimensions to maintain the crystalline lamellar structure of P(3HB) by the intermolecular-chain-packing.

Erosion Rate of PHA Single Crystals Determined by Real-Time AFM. Real-time AFM observations were carried out to obtain the dynamic information of the changes in morphology of PHA single crystals during enzymatic degradation. Figure 3 shows typical real-time AFM height images of L−P(3HB) single crystals during enzymatic degradation. As shown in Figure 3A, the single crystals of L−P(3HB) with 6.1 nm thickness were observed before enzymatic degradation in a buffer solution. Enzymatic erosions proceeded at the edges (*ac* plane) and ends (*bc* plane) of single crystals, and the fibril-like crystals were apparently generated by degradation over time by the action of PHB depolymerase, as reported previously.[16−23]

The grooves were formed along the crystallographic *a* axis, and the erosions of fibril-like crystals were progressed from both the tip of crystals along the *a* axis and the edges along the *b* axis. The eroded distances at the tip and edge of fibril-like crystals and at the point of grooves were determined from the real-time AFM images by measuring distances from the fixed spot in the images to the edges and ends of eroding crystals. Figure 4 shows the time-dependent changes in eroded distances at the root and tip of PHA fibril-like crystals. The eroded distances along the *a* axis at the root and along the *b* axis at the tip of fibril-like crystals were changed linearly with time at an early stage of enzymatic reaction. In contrast, the erosions along the *a* axis at the tip of fibril-

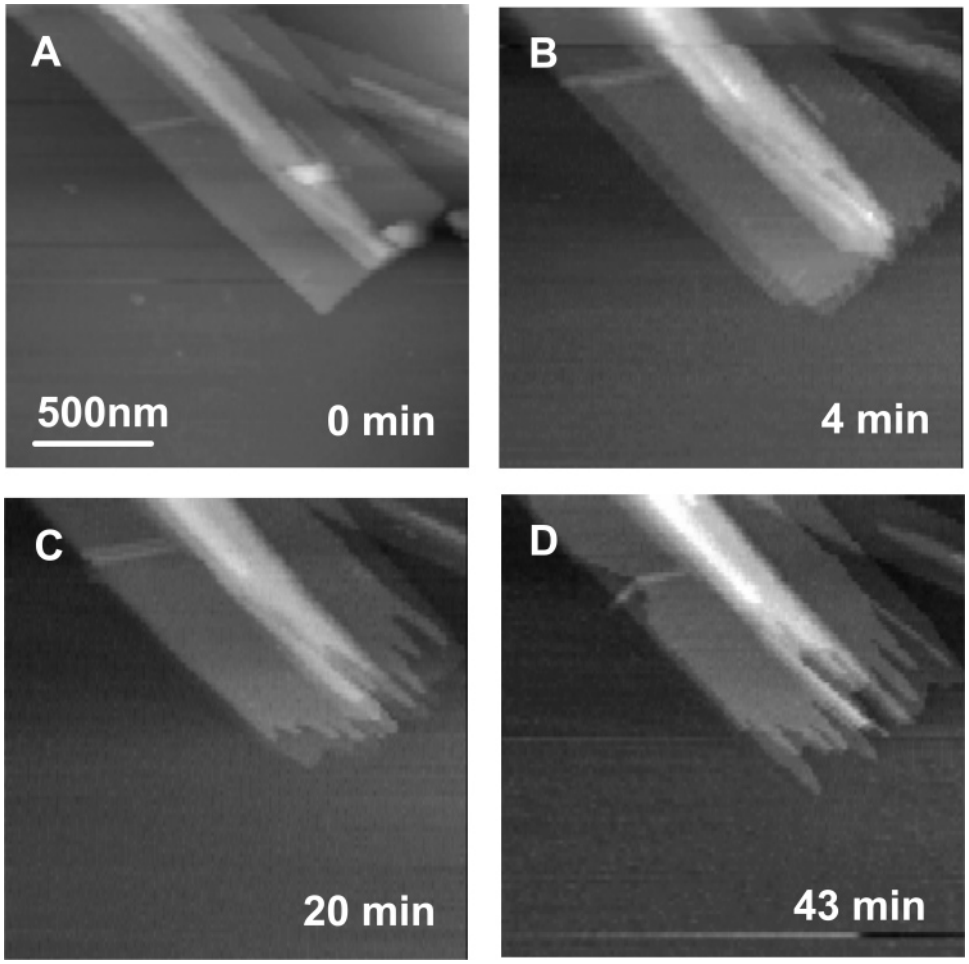

Figure 3. Real-time AFM height images of L−P(3HB) single crystals before (A) and during enzymatic degradation over time by PHB depolymerase at 37 °C (B−D). The first frame (A) was taken in a phosphate buffer solution at 37 °C.

like crystals started after the induction period, and then the erosion distances increased linearly with time. Enzymatic erosion rates in single crystals were calculated from the slope of the line plotting the eroded distance against time.

Table 3 lists the erosion rates at the tip and edge of fibril-like crystals and the point of grooves and overall erosion rates of PHA single crystals. For H−P(3HB), the grooves grew along the crystallographic *a* axis at the rate of 3.7 nm/min. The fibril-like crystals were eroded from the tip of crystals along the *a* axis at the rate of 2.6 nm/min and from the edges along the *b* axis at the rate of 1.3 nm/min. For the single crystals of P(3HB) with different molecular weights, the erosion rate at the point of the grooves along the *a* axis increased from 3.7 to 10.6 nm/min as the molecular weight of P(3HB) was decreased from 240 000 to 8500, whereas those at the tip of fibril-like crystals along the *a* and *b* axes revealed relatively similar values ranging from 2.6 to 3.8 and 1.1 to 1.3 nm/min, respectively, as independent of molecular weight. As shown in Table 3, for P(3HB-*co*-3HV) samples, both the erosion rates at the point of the grooves and at the tip of fibril-like crystals along the *a* axis increased significantly with an increase in the 3HV composition, whereas the rates at the edges along the *b* axis were slightly increased by the introduction of 3HV units.

Furthermore, we estimated the enzymatic erosion rate of PHA single crystals from the volumetric analysis by using real-time AFM height images. By considering the density of the P(3HB) crystalline region, the changes in volume of single crystals during enzymatic degradation can be converted into the weight changes. Scanned volumes of single crystals in AFM images were varied with individual samples. So, we had to normalize the changes in volume of single crystals by enzymatic degradation in a unit area on volume of crystal. Since PHB depolymerase predominantly hydrolyzes the polymer chains at the end (*bc* plane) of the single crystal, not from the chain-folding surface (*ab* plane), the weight changes of single crystals were normalized to a unit area of the crystal end. The unit area of crystal end (*bc* plane) was calculated from the width and thickness of single crystal observed in AFM images for crystals before degradation. Figure 5 shows the time-dependent changes in erosion weight of a PHA single crystals during enzymatic degradation. The erosion weight of PHA crystals increased linearly with degradation time. The overall degradation rate of PHA single crystals was determined from the slope of the line, and the values are listed in Table 3. The values of overall erosion rates from AFM measurement were comparable to the enzymatic erosion rate of melt-crystallized film reported by Abe et al.,[26] implying that we succeeded in analyzing the overall erosion rate of PHA single crystal during enzymatic degradation by real-time AFM observation. For P(3HB) single crystals, the overall erosion rates increased with a decrease in the molecular weight of P(3HB), similar to the erosion rate at the grooves. The overall degradation rates of

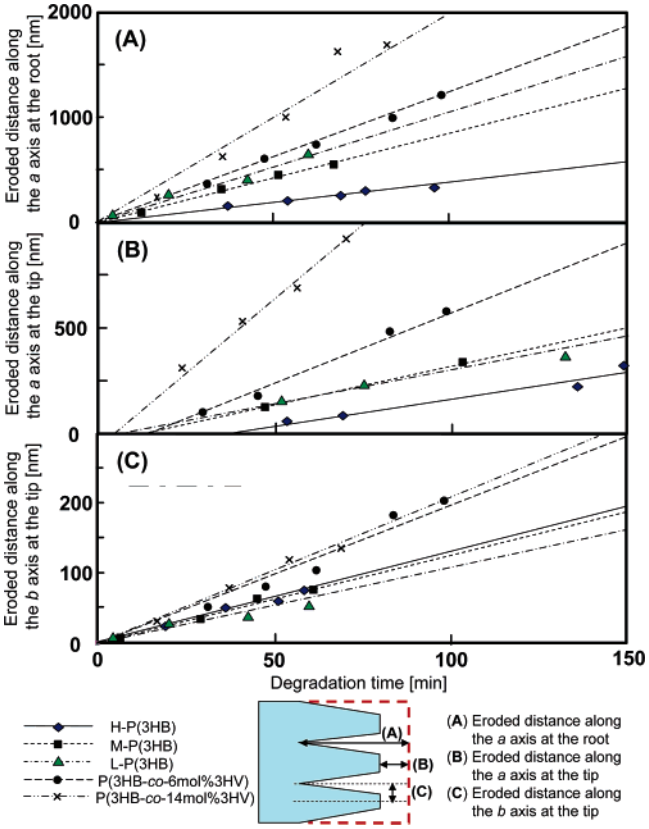

Figure 4. Time-dependent changes in erodeed distance along the crystallographic *a* axis at the root (A) and along the *a* and *b* axes at the tip (B and C) of the fibril-like crystal in PHA single crystals, respectively. The data in the graphs were calculated from the real-time AFM images during enzymatic degradation by PHB depolymerase at 37 °C. The illustration under the three graphs represents the kind of eroded distance in a lamellar crystal as shown in vertical axis of each graph.

Table 3. Partial and Overall Erosion Rates along *a* and *b* Axes at the Tip and Root of the Fibril-Like Crystals in PHA Single Crystals during Enzymatic Degradation

	erosion rates[a], nm/min			overall erosion rates, mg/(min cm^2)
	root	tip		
sample	*a* axis	*a* axis	*b* axis	
H−P(3HB)	3.7	2.6	1.3	0.0007
M−P(3HB)	8.3	3.8	1.3	0.0015
L−P(3HB)	10.6	3.2	1.1	0.0018
P(3HB-*co*-6 mol % 3HV)	12.4	6.8	2.0	0.0026
P(3HB-*co*-14 mol % 3HV)	19.7	14.1	2.1	0.0065

[a] Erosion rates were determined from real-time AFM observation like Figure 4.

P(3HB-*co*-3HV) single crystals were much faster than those of P(3HB) single crystals.

Discussion

Enzymatic Degradation Mechanism of Fibril-Like Crystals in PHA Single Crystals. Based on the AFM observations, it was confirmed that single crystals were eroded and slit along the long axis of the crystal from the edges and ends, generating fibril-like crystals were generated along the crystallographic *a* axis, as reported previously.[16−23] The thickness at the root of fibril-like crystals was almost

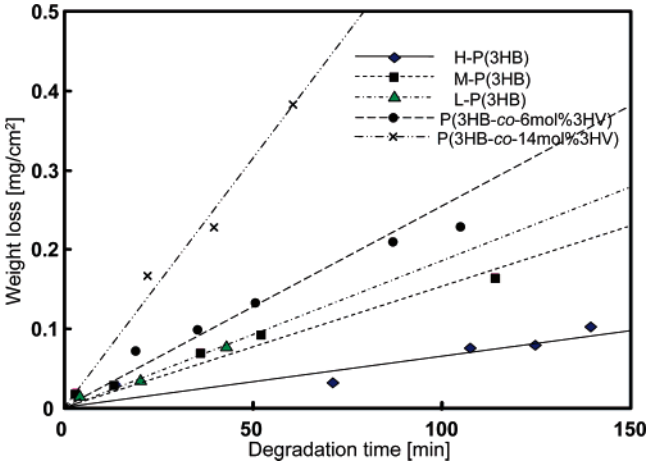

Figure 5. Enzymatic erosion profiles in the weight degraded PHA single crystals by PHB depolymerase at 37 °C. The data in this graph were calculated from the degraded volume measured by the real-time AFM images.

the same as the thickness of original single crystals after enzymatic degradation for 1 h at 37 °C. Previously, Iwata et al. reported that the molecular weights of P(3HB) molecules were almost unchanged during enzymatic degradation, suggesting that the enzymatic hydrolysis took place only at the edges and ends of crystals, not at chain-folding surface.[20] However, it was found that the thickness at the tip of fibril-like crystals was apparently thinner than the thickness of single crystals before degradation in this study. Iwata et al. also reported that PHB depolymerase adsorbed unselectively on the crystalline surface and degraded lamellar crystal along the crystallographic *a* axis from the crystal edges and ends.[18−20] Murase et al. found that the slits and crevices were formed on the P(3HB) single crystals during enzymatic reaction by using hydrolytic-activity-disrupted mutant of the enzyme.[23] They suggested that the adsorption of PHB depolymerase onto the crystalline surface distorted the molecular packing of P(3HB) single crystals.[23]

From these results, we have proposed an enzymatic degradation mechanism of fibril-like crystals generated from PHA single crystals, as shown in Figure 6. In the PHA single crystals, both the ordered and disordered chain-packing regions may exist alternatively with periodic intervals due to the crystallization characteristic of P(3HB) molecules (Figure 6A). PHB depolymerase adsorb homogeneously on the edges, ends and chain-folding crystalline surfaces. The adsorbed enzymes predominantly hydrolyze the polymer molecules at the disordered chain-packed regions in single crystals from the edges and ends, as shown in Figure 6B. As a result, the ordered chain-packing regions have remained as fibril-like crystals (Figure 6, panels C and D). Figure 6E demonstrates that the enzymes adsorbed on the fibril-like crystals also erode the ordered chain-packing region from the edge, and the fibril-like crystals become narrow up to a minimum value (around 28 nm). In addition, the adsorption of enzyme on the fibril-like crystals may induce the enhancement of molecular mobility in ordered chain-packing regions. And then, the molecular packing structure of ordered chain-packing region is gradually distorted with time from the chain-folding surface along the crystallographic *c* axis to reach a minimum value (around 1.9 nm), as shown in Figure

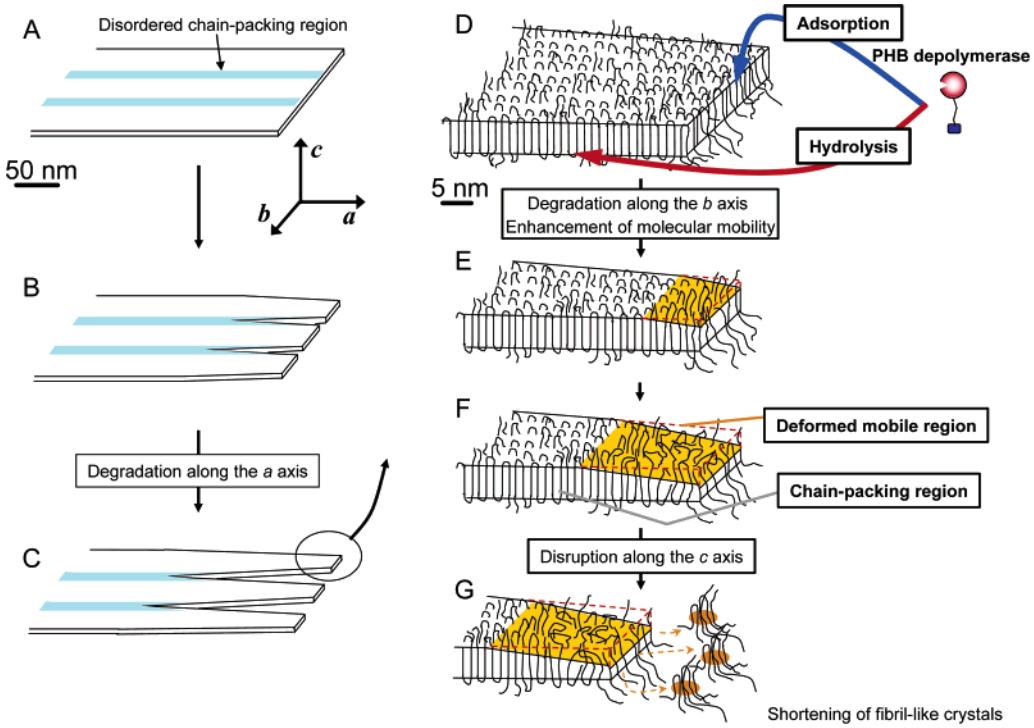

Figure 6. Schematic model of enzymatic degradation behavior of lamellar crystal in P(3HB) solution-grown single crystal by PHB depolymerase from *R. pickettii* T1 at 37 °C.

6F. In this study, we performed the tapping mode AFM for the dimensional analysis of PHA single crystal. Even with the tapping mode AFM measurement, it is difficult to avoid the penetration of the AFM cantilever tip into soft material such as amorphous polymer. The AFM cantilever tip may penetrate the distorted crystalline region on the chain-folding surface formed by the adsorption of PHB depolymerase, and the measured thickness may reflect the thickness of remaining ordered chain-packing regions. When the crystal dimensions fall below minimum values by the erosion from the edge and distortion from the chain-folding surface, it is difficult to keep the lamellar structure, such is as seen at the tip of the fibril-like crystal when it is collapsed such as the destruction shown in Figure 6G at the tip of the glacier. As a result, in Figure 6G, the fibril-like crystals are shortened by the disruption of the tip. Finally, the chips formed by the destruction at the tip are hydrolyzed to water-soluble dimers and monomers by PHB depolymerase.

Influence of Molecular Weight of P(3HB) on Erosion Rate and Morphology of Fibril-Like Crystals. From the real-time AFM observations, the erosion rates at different points of single crystals could be determined for P(3HB) samples with different molecular weights. As can be seen in Table 3, the erosion rate along the *a* axis at the grooves was obviously dependent on the molecular weight. As mentioned above, the formation of grooves was attributed to the degradation of disordered chain-packing region in single crystals. As the molecular weight of P(3HB) is decreased, the number of the chain ends increases on the crystalline surface. With an increase in chain end groups, the disordered chain-packing region may become more unstable. In addition, PHB depolymerase easily hydrolyzes the P(3HB) molecules from the chain ends exposed on the surface of single crystal. Therefore, the erosion rate at the grooves (disordered chain-packing region) increased with a decrease in molecular weight of P(3HB). In contrast, the erosion rates along the *a* and *b* axes at the tip of fibril-like crystals had similar, independent of the molecular weight, for all P(3HB) samples. The fibril-like crystals all consist of the highly ordered chain-packing region. In addition, the erosion rate along the *a* axis of fibril-like crystals reflected the destruction rate at the tip of the crystals. The packing structure of such highly ordered crystalline regions may be slightly influenced by the numbers of chain-foldings and chain ends.

As shown in Table 2, the morphology of fibril-like crystal formed after enzymatic degradation for 1 h varied with the molecular weight of P(3HB). The length of fibril-like crystals became smaller in the following order: L−P(3HB) > M−P(3HB) > H−P(3HB). The erosion rates at the grooves of P(3HB) single crystals increased with a decrease in molecular weight, whereas the erosion rates at the tip of fibril-like crystals were almost same value. In addition, the erosion rates at the grooves of P(3HB) single crystals were larger than those at the tip of fibril-like crystals. Therefore, the fibril-like crystals were getting longer with degradation time. Therefore, we have concluded that the length of fiberil-like crystals is governed by the ratio of the erosion rates between at the grooves and at the tip of crystals. Indeed, the length of fibril-like crystals for the L−P(3HB) sample determined from static AFM observations was in good agreement with the value calculated from the difference in the erosion rates between the grooves and at the tip of crystals. For the H−P(3HB) sample, the erosion rates at the grooves and at the tip of crystals revealed relatively closed values, whereas the fibril-like crystals were formed sufficiently long after degradation for 1 h as shown in Table 1. As shown in Figure 4, the erosion at the tip of fibril-crystals

for H−P(3HB) samples started after an induction time. By considering the presence of the induction of erosion time, the length of fibril-like crystals was in fair agreement with the calculated value from the erosion rates between at the grooves and at the tip of crystals.

Effect of 3HV Composition on Erosion Rate and Morphology of Fibril-Like Crystals. The crystal structure of random copolymers of 3HB and 3HV has been investigated extensively.[27−29] It has been reported that the P(3HB-*co*-3HV) copolymers show isodimorphism due to the cocrystallization of 3HB and 3HV units in a composition range from 0 to 27 mol % of 3HV units.[29] As shown in Table 3, both the erosion rates at the grooves and at the tip of fibril-like crystal for the P(3HB-*co*-3HV) single crystal were apparently larger than those of the P(3HB) single crystals. In addition, each value increased with an increase in the 3HV composition. These results suggest that 3HV units are incorporated into the single crystals. Such isodimorphic crystals of P(3HB-*co*-3HV) may be more unstable than pure P(3HB) crystals, which reflects the melting temperature depression of the P(3HB-*co*-3HV) copolymer. Thus, in more facile erosion by PHB, depolymerase was observed in the P(3HB-*co*-3HV) single crystals than in the P(3HB) single crystals.

Although the erosion rates of P(3HB-*co*-3HV) single crystals were accelerated with increasing 3HV content, the average lengths of fibril-like crystals for P(3HB-*co*-3HV) samples were shorter than those of P(3HB) samples (see Table 2). As shown in Table 3, the difference of erosion rates between the grooves and tip of fibril-like crystals for P(3HB-*co*-3HV) was slightly smaller than that of P(3HB). In addition, the induction period starting the erosion of fibril-like crystals for P(3HB-*co*-3HV) was shorter than that of P(3HB) (see Figure 5). Therefore, the lengths of fibril-like crystals for P(3HB-*co*-3HV) samples became shorter than those of P(3HB) samples.

Conclusions

The enzymatic degradation processes of five types of PHA (H−P(3HB), M−P(3HB), L−P(3HB), P(3HB-*co*-6mol % 3HV), and P(3HB-*co*-14mol % 3HV)) single crystals by PHB depolymerase from *R. pickettii* T1 were studied by AFM observations. After enzymatic degradation, fibril-like crystals with periodical intervals were generated from PHA single crystals, and the morphologies and sizes of fibril-like crystals were found to depend on both the molecular weight and copolymer composition of PHA samples. The erosion rates of single crystals were determined from the real-time AFM images. The enzymatic erosion of the disordered chain-packing region started at the initial stage of degradation. The erosion rate along the *a* axis at the grooves increased with a decrease of molecular weight and with an increase of 3HV content. The generated fibril-like crystals eroded along both the *a* and *b* axes. The erosion along the *a* axis at the tip of fibril-like crystals progressed with a constant rate after the induction time, and the erosion rate was smaller than the erosion rate at the grooves. In addition, it was found that the crystalline thickness of the fibril-like crystal gradually decreased toward a tip from the root of the crystal, suggesting that the deformation of the fibril-like crystal along the *c* axis took place during the degradation. The adsorption of enzyme on the chain-folding surface may induce the destruction of the chain-packing structures of the fiberl-like crystals toward the *c* axis. The erosion rate along the *a* axis at the tip of fibril-like crystal is related to the thinning process of the crystal, and the destruction rate along the *c* axis is affected by the chain-packing structure. Therefore, the erosion rate along the *a* axis at the tip of the fibril-like crystal increased with 3HV composition due to the isodimorphic crystals of P(3HB-*co*-3HV). The morphologies and sizes of fibril-like crystals were established by both the erosion rates along the *a* axis at the grooves and tip of the fibril-like crystals. Furthermore, it was confirmed that the overall enzymatic erosion rate of single crystals by PHB depolymerase, determined from the volumetric analysis, was comparable to the erosion rate obtained from the enzymatic degradation of melt-crystallized PHA films.

Acknowledgment. This work has been supported by SORST (Solution Oriented Research for Science and Technology) from Japan Science and Technology Agency (JST) and the grant of Ecomolecular Science Research from RIKEN Institute.

References and Notes

(1) Doi, Y. *Microbial Polyesters*; VCH Publishers: New York, 1990.
(2) Doi, Y., Steinbüchel, A., Eds.; *Biopolymers, Vol. 3, Polyesters I and II*; Wiley-VCH: Weinheim, Germany, 2001.
(3) Sudesh, K.; Abe, H.; Doi, Y. *Prog. Polym. Sci.* **2000**, *25*, 1503.
(4) Alper, R.; Lundgren, D. G.; Marchessault, R. H.; Cote, W. A. *Biopolymers* **1963**, *1*, 545.
(5) Okamura, K.; Marchessault, R. H. *Conformation of Biopolymers*; Ramachandran, C. N., Ed., Academic Press: New York, 1967; Vol. 2, p 709.
(6) Cornibert, J.; Marchessault, R. H. *J. Mol. Biol.* **1972**, *71*, 735.
(7) Yokouchi, M.; Chatani, H.; Tadokoro, H.; Teranishi, K.; Tani, H. *Polymer* **1973**, *14*, 267.
(8) Brückner, S.; Meille, S. V.; Malpezzi, L.; Cesaro, C.; Navarini, L.; Tombolini, R. *Macromolecules* **1988**, *21*, 967.
(9) Tanio, T.; Fukui, T.; Shirakura, Y.; Saito, T.; Tomita, K.; Kaiho, T.; Masamune, S. *Eur. J. Biochem.* **1982**, *124*, 71.
(10) Mukai, K.; Yamada, K.; Doi, Y. *Int. J. Biol. Macromol.* **1992**, *14*, 235.
(11) Mergaert, J.; Webb, A.; Anderson, C.; Wouters, A.; Swings, J. *Appl. Environ. Microbiol.* **1993**, *59*, 3233.
(12) Jendrossek, D.; Schirmer, A.; Schlegel, H. G. *Appl. Microbiol. Biotechnol.* **1996**, *46*, 451.
(13) Kikkawa, Y.; Fujita, M.; Hiraishi, T.; Yoshimoto, M.; Doi, Y. *Biomacromolecules* **2004**, *5*, 1642.
(14) Abe, H.; Mastubara, I.; Doi, Y. *Macromolecules* **1995**, *28*, 844.
(15) Hocking, P. J.; Marchessault, R. H.; Timmins, M. R.; Lenz, R. W.; Fuller, R. C. *Macromolecules* **1996**, *29*, 2472.
(16) Nobes, G. A. R.; Marchessault, R. H.; Chanzy, H.; Briese, B. H.; Jendrossek, D. *Macromolecules* **1996**, *29*, 8330.
(17) Nobes, G. A. R.; Marchessault, R. H.; Briese, B. H.; Jengrossek, D. *J. Environ. Polym. Degrad.* **1998**, *6*, 99.
(18) Iwata, T.; Doi, Y.; Kasuya, K.; Inoue, Y. *Macromolecules* **1997**, *30*, 833.
(19) Iwata, T.; Doi, Y.; Tanaka, T.; Akehata, T.; Shiromo, M.; Teramachi, S. *Macromolecules* **1997**, *30*, 5290.
(20) Iwata, T.; Doi, Y.; Nakayama, S.; Sasatsuki, H.; Teramachi, S. *Int. J. Biol. Macromol.* **1999**, *25*, 169.
(21) Murase, T.; Iwata, T.; Doi, Y. *Macromolecules* **2001**, *34*, 5848.
(22) Murase, T.; Iwata, T.; Doi, Y. *Macromol. Biosci.* **2001**, *1*, 275.
(23) Murase, T.; Suzuki, Y.; Doi, Y.; Iwata, T. *Biomacromolecules* **2002**, *3*, 312.
(24) Numata, K.; Hirota, T.; Kikkawa, Y.; Tsuge, T.; Iwata, T.; Abe, H.; Doi, Y. *Biomacromolecules* **2004**, *5*, 2186.

(25) Shirakura, Y.; Fukui, T.; Saito, T.; Okamoto, Y.; Narikawa, T.; Koide, K.; Tomita, K.; Takemasa, T.; Masamune, S. *Biochim. Biophys. Acta.* **1986**, *880*, 46.
(26) Abe, H.; Doi, Y.; Aoki, H.; Akehata, T. *Macromolecules* **1998**, *31*, 1791.
(27) Bluhm, T. L.; Hamer, G. K.; Marchessault, R. H.; Fyfe, C. A.; Veregin R. P. *Macromolecules* **1986**, *19*, 2871.
(28) Kamiya, N.; Sakurai, M.; Inoue, Y.; Chujo, R. *Macromolecules* **1991**, *24*, 3888.
(29) VanderlHart, D. L.; Orts, W. J.; Marchessault, R. H. *Macromolecules* **1995**, *28*, 6394.

BM0501151